Benajes Calvo, JV.; Pastor Soriano, JV.; García Martínez, A.; Monsalve Serrano, J. (2015). An experimental investigation on the influence of piston bowl geometry on RCCI performance and emissions in a heavy-duty engine. Energy Conversion and Management. 103:1019-1030. doi:10.1016/j.enconman.2015.07.047.

An experimental investigation on the Influence of piston bowl geometry on RCCI performance and emissions in a heavy-duty engine

Energy Conversion and Management, Volume 103, October 2015, Pages 1019-1030.
http://dx.doi.org/10.1016/j.enconman.2015.07.047

Jesús Benajes, José V. Pastor, Antonio García*, Javier Monsalve-Serrano

CMT - Motores Térmicos, Universitat Politècnica de València, Camino de Vera s/n, 46022 Valencia, Spain

(*) Corresponding author: angarma8@mot.upv.es (Antonio García Martínez)

Abstract

This experimental work investigates the effects of piston bowl geometry on RCCI performance and emissions at low, medium and high engine loads. For this purpose three different piston bowl geometries with compression ratio 14.4:1 have been evaluated using single and double injection strategies. The experiments were conducted in a heavy-duty single-cylinder engine adapted for dual fuel operation. All the tests were carried out at 1200 rev/min.

Results suggest that piston geometry has great impact on combustion development at low load conditions, more so when single injection strategies are used. It terms of emissions, it was proved that the three geometries enables ultra-low NOx and soot emissions at low and medium load when using double injection strategies. By contrast, unacceptable emissions were measured at high load taking into account EURO VI limitations. Finally, the application of a mathematical function considering certain self-imposed constraints suggested that the more suitable piston geometry for RCCI

operation is the stepped one, which has a modified transition from the center to the squish region and reduced piston surface area than the stock geometry.

Keywords

Reactivity Controlled Compression Ignition; EURO VI; Efficiency; Dual fuel; Combustion

1. Introduction

As response of the regulations introduced around the world to limit the pollutant emissions associated to internal combustion engines, researchers and manufacturers are focusing their efforts on develop new combustion strategies and aftertreatment systems to fulfill the stringent limitations. Since the complex aftertreatment devices incur in higher costs and fuel consumption, the in-cylinder emissions reduction is clearly necessary.

Homogeneous charge compression ignition (HCCI), a widely investigated LTC combustion concept, has demonstrated great potential to produce virtually no soot and NOx emissions while maintaining high efficiency [1][2][3]. By contrast, new challenges regarding combustion control and mechanical engine stress were identified [4]. Thus, Bessonette et al. [5] suggested that different in-cylinder reactivity is required for proper HCCI operation under different operating conditions. In particular, high cetane fuels are required at low load and a low cetane fuels are needed at medium-high load. With the aim of improving controllability and reduce the knocking level in HCCI combustion, the use of gasoline-like fuels under partially premixed combustion (PPC) strategies has been widely studied [6-12]. The investigations confirmed gasoline PPC as promising method to control the heat release rate while providing a simultaneous reduction in NOx and soot emissions [13][14]. However, the concept demonstrated difficulties at low load conditions using gasoline with octane number

(ON) greater than 90 [15][16]. In this sense, the spark assistance provided temporal and spatial control over the gasoline PPC combustion process [17][18][19], but resulted in unacceptable NOx and soot emissions [20], even using double injection strategies [21][22].

Recent experimental and simulated studies proved that reactivity controlled compression ignition (RCCI), a dual-fuel diesel-gasoline combustion concept, is more promising LTC technique than HCCI and PPC [23][24]. Thus, RCCI concept allows an effective control of in-cylinder equivalence ratio and reactivity stratification [25][26] through the gasoline fraction and direct injection timing variation [27-30]. That flexibility allows ultra-low NOx and soot emission levels with improved fuel consumption than conventional diesel combustion (CDC) in a wide engine operating range [31]. However, it was also found that HC and CO emissions levels from RCCI concept are considerably higher than CDC, overall at low load operation.

Several strategies has been studied to minimize RCCI combustion losses. In this sense, the combination of different engine settings, such as in-cylinder gas temperature and oxygen concentration with gasoline fraction, was confirmed as potential way to rise combustion efficiency values above 98% [32]. Moreover, an effective conversion of CO and HC emissions from RCCI at exhaust temperatures greater than 300 °C was proved with several diesel oxidation catalysts (DOC) [33]. Another strategy widely studied is the use of renewable oxygenated fuels, such as ethanol [34-37]. In all cases, E85 fuel increased CO and HC emissions while NOx and soot emission decreased simultaneously in most of the cases. In addition, physicochemical properties of E85 resulted in a particular combustion behavior with narrow operating range, limited by misfire and excessive knocking at low and high load, respectively. By contrast, minor portions of

ethanol (10%-20%) showed clear potential to reach EURO VI NOx and soot levels with improved HC and CO emissions from low to high load [38].

Finally, the influence of piston geometry on RCCI emissions and efficiency in a heavy-duty engine has been also studied in literature. Thus, computational results identified crevices and squish volumes as primary sources of incomplete combustion. In addition, these findings were proved experimentally up to medium load using various piston geometries with different compression ratios and E85 as low reactivity fuel [39]. In other work [40], the most suitable geometry from [39], was directly compared to the stock re-entrant geometry at the same compression ratio of 17.4:1 in a high-speed engine working under RCCI conditions. In this case, it was found that the modified RCCI piston allowed a 2 to 4% absolute improvement in gross indicated efficiency, which was attributed to both, combustion efficiency gains and a reduction in the heat transfer losses. In addition, the modified RCCI piston resulted in higher NOx emissions due to the higher combustion temperature peaks. Based on these results, the current research focuses on evaluate two new geometries, aimed to modify the squish flow and also to reduce heat transfer losses, operating under RCCI combustion from low to high load in a heavy-duty engine. To allow direct comparison, both geometries have been designed with the same nominal compression ratio than the stock piston (CR=14.4:1). Thus, to compare the three geometries, experimental tests were conducted in a heavy-duty diesel engine at 1200 rev/min using single and double injection strategies. Finally, a mathematical function has been used to select the proper piston geometry for RCCI operation according to certain self-imposed constraints.

2. Materials and methods

2.1. Single-cylinder engine, fuels and test cell description

A single-cylinder diesel engine, representative of commercial truck engine, has been used in this study. The major difference to the standard unit production is the hydraulic VVA system, which conferred great flexibility during the research. In particular, the valve timing, duration and lift can be electronically controlled for each valve during the engine tests. Thus, an adapted cylinder head to include a dedicated oil circuit is required. Detailed specifications of the engine are given in Table 1.

Table 1. Single cylinder engine specifications.

Engine type	Single cylinder, 4 St cycle, DI
Bore x Stroke [mm]	123 x 152
Connecting rod length [mm]	225
Displacement [L]	1.806
Geometric compression ratio [-]	14.4:1
Bowl Type	Open crater
Number of Valves	4
Rated power @ 1200 rpm [kW]	41
IVO	375 CAD ATDC
IVC	535 CAD ATDC
EVO	147 CAD ATDC
EVC	347 CAD ATDC

To enable RCCI operation the engine was equipped with a double injection system, one for each fuel used. This injection hardware enabled to vary the in-cylinder fuel blending ratio and fuel mixture properties according to the engine operating conditions. Thus, to inject the diesel fuel, the engine was equipped with a common-rail flexible injection hardware which is able to perform up to five injections per cycle. The main characteristic of this hardware is its capability to amplify common-rail fuel pressure for one of the injection events by means of a hydraulic piston directly installed inside the injector. Concerning the gasoline injection, an additional fuel circuit was in-house built including a reservoir, fuel filter, fuel meter, electrically driven pump, heat exchanger and commercially available port fuel injector (PFI). The mentioned injector was located at

the intake manifold and was specified to be able to place all the gasoline fuel into the cylinder during the intake stroke. Consequently, the gasoline injection timing was fixed 10 CAD after the IVO to allow the fuel to flow along 160 mm length (distance from PFI location to intake valves seats). Accordingly, this set-up avoided fuel pooling over the intake valve and the undesirable variability introduced by this phenomenon. The main characteristics of the diesel and gasoline injectors are depicted in Table 2.

Table 2. Diesel and gasoline fuel injector characteristics.

Diesel injector		Gasoline injector	
Actuation Type	Solenoid	Injector Style	Saturated
Steady flow rate @ 100 bar [cm^3/s]	28.56	Steady flow rate @ 3 bar [cm^3/s]	980
Number of Holes	7	Included Spray Angle [°]	30
Hole diameter [um]	194	Fuel Pressure [bar]	5.5
Included Spray Angle [°]	142	Start of Injection [CAD aTDC]	385

To carry out the experimental tests, commercially available diesel and 98 ON gasoline fuels were selected as high and low reactivity fuel, respectively. Their main properties are listed in Table 3.

Table 3. Physical and chemical properties of the fuels used along the study.

	Gasoline	Diesel
Density [kg/m^3] (T= 15 °C)	772	882
Viscosity [mm^2/s] (T= 40 °C)	0.37	2.8
Octane number [-]	98	-
Cetane number [-]	-	52
Lower heating value [kJ/kg]	44.542	42.651

The engine was installed in a fully instrumented test cell, with all the auxiliary facilities required for its operation and control, as it is illustrated in Figure 1. In addition, Table 4 summarizes the accuracy of the instrumentation used in this work.

Table 4. Accuracy of the instrumentation used in this work.

Variable measured	Device	Manufacturer / model	Accuracy
In-cylinder pressure	Piezoelectric transducer	Kistler / 6125B	±1.25 bar
Intake/exhaust pressure	Piezorresistive transducers	Kistler / 4045A10	±25 mbar
Temperature in settling chambers and manifolds	Thermocouple	TC direct / type K	±2.5 °C
Crank angle, engine speed	Encoder	AVL / 364	±0.02 CAD
NOx, CO, HC, O_2, CO_2	Gas analyzer	HORIBA / Mexa 7100 DEGR	4%
FSN	Smoke meter	AVL / 415	±0.025 FSN
Gasoline/diesel fuel mass flow	Fuel balances	AVL / 733S	±0.2%
Air mass flow	Air flow meter	Elster / RVG G100	±0.1%

The in-cylinder pressure was measured with a Kistler 61215C pressure transducer coupled with a Kistler 5011B10 charge amplifier. A shaft encoder with 1800 pulses per revolution was used, which supplied a resolution of 0.2 CAD.

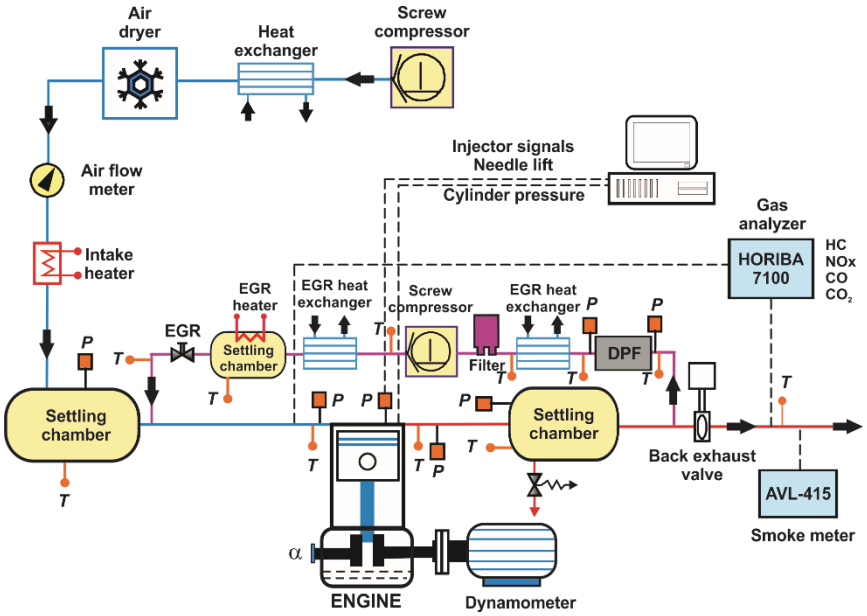

Figure 1. Complete test cell setup.

Moreover, to achieve stable intake air conditions, a screw compressor supplied the required boost pressure before passing through an air dryer. The air pressure was adjusted within the intake settling chamber, while the intake temperature was controlled in the intake manifold after mixing with the EGR flow. The exhaust

backpressure produced by the turbine in the real engine was replicated by means of a valve placed in the exhaust system, controlling the pressure in the exhaust settling chamber. Low pressure EGR was produced taking exhaust gases from the exhaust settling chamber. Thus, the determination of the EGR rate was carried out using the experimental measurement of intake and exhaust CO_2 concentration. The concentrations of NOx, CO, unburned HC, intake and exhaust CO_2, and O_2 were analyzed with a five gas Horiba MEXA-7100 DEGR analyzer bench by averaging 40 seconds after attaining steady state operation. CO and unburned HC measurements were used to determine the combustion efficiency as:

$$\text{Comb. Eff} = \left(1 - \frac{\text{HC}}{\text{m}_f} - \frac{\text{CO}}{4 \cdot \text{m}_f}\right) \cdot 100 \quad (1)$$

Where HC accounts the mass of unburned hydrocarbon emissions, CO is the mass of carbon monoxide and m_f is the total fuel mass injected.

Smoke emission were measured with an AVL 415S Smoke Meter and averaged between three samples of a 1 liter volume each with paper-saving mode off, providing results directly in FSN (Filter Smoke Number) units. PM measurements of FSN were transformed into specific emissions (g/kWh) by means of the factory AVL calibration.

2.2. Piston bowl geometries

As identified in introduction section, fuel consumption and combustion losses are potential areas for RCCI optimization. Thus, two bowl geometries aimed to reduce unburned HC and CO accumulation within the squish region as well as to mitigate heat transfer losses, were designed and evaluated by means of experimental tests.

The first geometry, shown in Figure 2, was named as steeped and maintains the stock piston central shape with modified transition from the piston head to the squish

region. The purpose of this geometry was to modify the squish flow in order to enhance unburned products oxidation in this zone. Stepped geometry resulted in 4.6% lower piston surface than stock piston, which should limit heat transfer [41]. The second geometry was named as bathtub due to its similitude to the piston used in [40], but it is worthy to note that the central part of the piston used in the current work is not completely flat as in previous literature is. This design also aimed to modify the squish flow, but with greater reduction in piston surface area (16% lower than stock piston) for lowering heat transfer losses. Further reduction in piston surface area was not possible due to structural constraints of the available piston blanks. It is interesting to remark that both geometries kept constant the geometric compression ratio of the stock piston, CR=14.4:1.

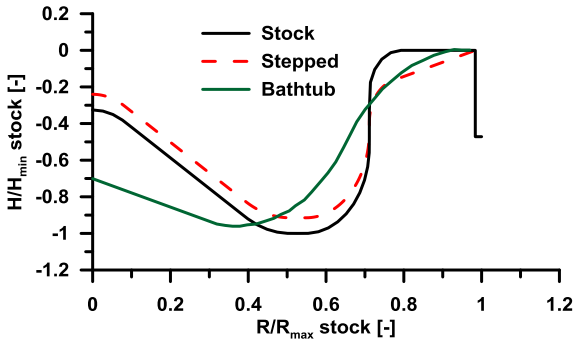

Figure 2. Stock, stepped and bathtub piston geometries.

2.3. Combustion diagnosis tool: CALMEC

The combustion analysis was performed by means of an in-house one-zone model named CALMEC, which is fully described in [42]. This combustion diagnosis tool used the in-cylinder pressure signal as its main input. Thus, the pressure traces from 150 consecutive engine cycles were recorded in order to compensate the cycle-to-cycle variation during engine operation. Later, each individual cycle's pressure data was smoothed using a Fourier series low-pass filter. Once filtered, the collected cycles were ensemble averaged to yield a representative cylinder pressure trace, which was used to

perform the analysis. Then, the first law of thermodynamics was applied between IVC and EVO, considering the combustion chamber as an open system because of blow-by and fuel injection. In addition, the ideal gas equation of state was used to calculate the mean gas temperature in the chamber. The main results from the model used in this work are the rate of heat release (RoHR) as well as additional information related to each cycle. In particular, the IMEP, start of combustion (defined as the crank angle position in which the cumulated heat release has reached a value of 2%) and combustion phasing (defined as the crank angle position of 50% fuel mass fraction burned) were obtained, among other parameters. Additionally, ringing intensity was calculated by means of the correlation of Eng [43]:

$$RI = \frac{1}{2\gamma}\frac{[0.05 \cdot (dP/dt)_{max}]^2}{P_{max}}\sqrt{\gamma R T_{max}} \quad (2)$$

Where γ is the ratio of specific heats, $(dP/dt)_{max}$ is the peak PRR, P_{max} is the maximum of in-cylinder pressure, R is the ideal gas constant, and T_{max} is the maximum of in-cylinder temperature.

3. Results and discussion

3.1. Low load results

Table 5 (a) depicts the main operating conditions fixed and swept for the parametric studies at low load. In the case of double injection, the injection settings fixed during the diesel pilot and main injection sweeps are presented in parenthesis.

Table 5. Detail of the engine settings used for the parametric studies at low (a), medium (b) and high load (c).

Load [-]	Low (a)	Medium (b)	High (c)
Constant engine settings			
Speed [rpm]	1200	1200	1200
Air mass flow [kg/h]	53.3	86	118

Total fuel [mg/cycle]	70	119	175
Effective CR [-]	14.4	11	11
Intake pressure (bar)	1.35	2.2 to 2.96	3.4
Intake Temperature [°C]	40	40	32
YO_2 IVC [%]	15.5	15.1	16.3
Single injection			
Diesel IP [bar]	1000	1175	1890
Gasoline fraction [%]	65 to 85	60 to 70	50 to 75
Diesel SOI [CAD aTDC]	-15 to -24	-9 to -21	-6 to +6
Double injection			
Diesel IP [bar]	700	800	900
Gasoline fraction [%]	75	80	70
Diesel pilot [CAD aTDC]	-40 to -60 (-15)	-40 to -60 (-12)	-40 to -60 (-10)
Diesel main [CAD aTDC]	(-60) -25 to -40	(-60) -9 to -40	(-40) -4 to -16
Diesel ratio [%pilot/%main]	60/40	70/30	50/50

Figure 3 shows the emissions and combustion parameters versus the relative fuel consumption to CDC for the different sweeps proposed in Table 5 (a). Dashed lines across the figures denote EURO VI emissions limits for HD diesel engines. The effects of diesel injection timing and gasoline fraction (GF) are described in the CO emissions subfigure, based on bathtub results. Nonetheless, the behavior explained can be extrapolated to the other two geometries.

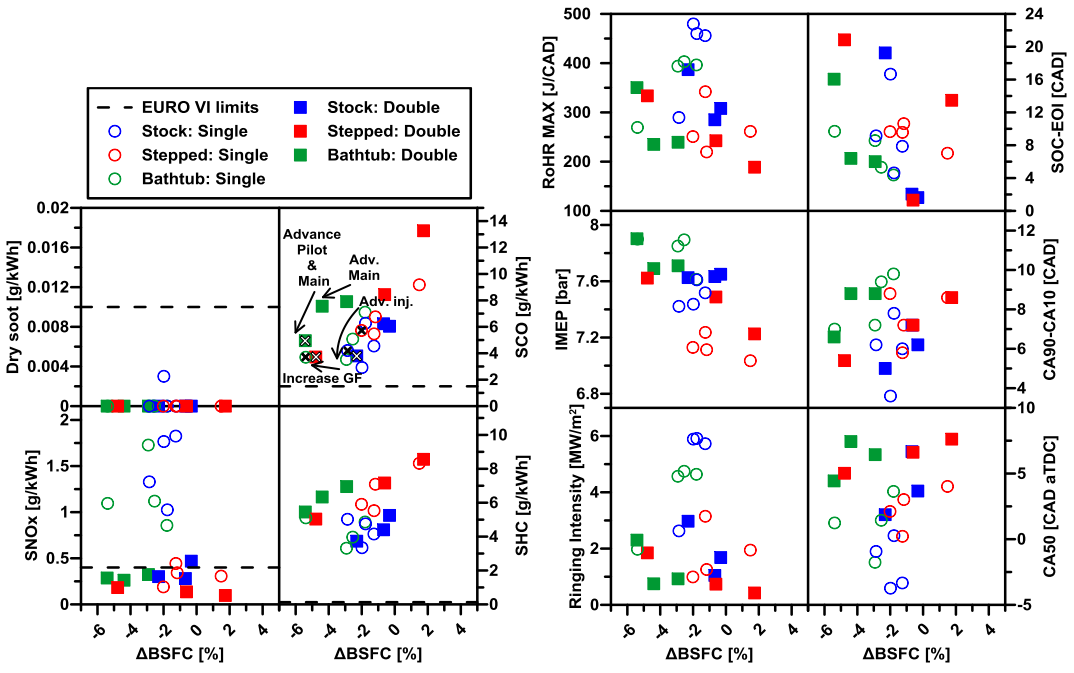

Figure 3. Emissions (left) and combustion parameters (right) for the three piston geometries at low load conditions versus the relative fuel consumption to CDC. Tests with single and double injection strategies are depicted.

In order to explain clearly the effects of injection timing and GF on combustion development, Figure 4 shows the RoHR and mean temperature for some specific cases of double and single injection strategies. For the sake of clarity, only the profiles of bathtub piston are presented, while the explanation is also valid for the other two geometries.

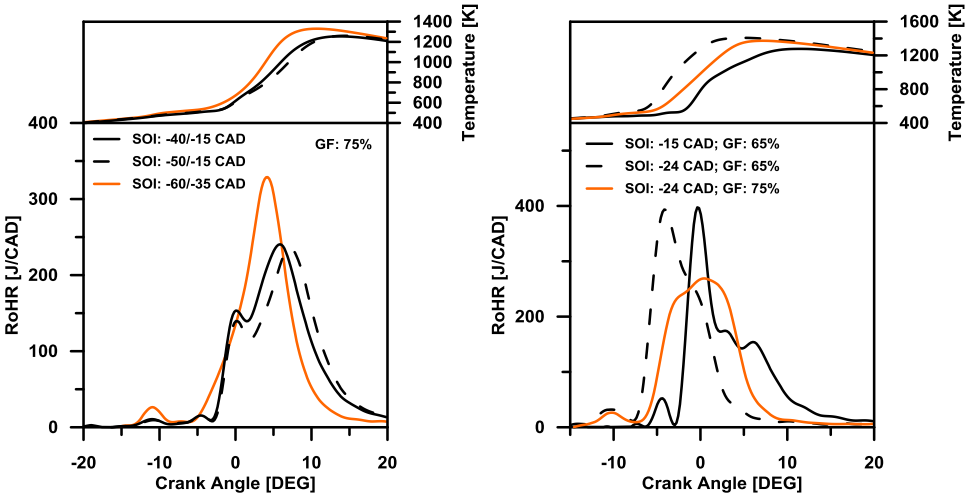

Figure 4. Experimental RoHR and mean temperature of the different sweeps with double (left) and single injection (right) for bathtub piston at low load conditions.

Focusing on double injection results, it is stated that an advance in pilot injection while keeping constant the main injection does not have a strong effect on combustion development. Thus, start of combustion (SOC) is equal in both cases, which denotes that main injection governs the combustion onset. In addition, a lower first RoHR peak and delayed combustion progression is observed for the most advanced strategy. This fact is well related to the higher mixing time available for the pilot injection, which results in leaner equivalence ratios at SOC. As the main injection is advanced together with the pilot one, the combustion pattern moves from two staged to one stage Gaussian-shaped heat release. This combustion shape results in improved HC and CO

emissions due to the enhanced RoHR peak and temperature, while maintaining NOx and soot levels below EURO VI limits. Moreover, the well-timed and fast heat release achieved promotes also an improvement in fuel consumption.

With respect to the single injection, a change in combustion pattern is also observed when advancing the diesel injection timing from -15 CAD to -24 CAD aTDC with the same GF. As seen from Figure 3, SOC-EOI is almost double for the most advanced case, which allows to reduce considerably the late combustion period after the premixed peak. In this sense, the advanced CA50 results in higher combustion temperatures leading to lower CO and HC with remarkable higher NOx. In addition, the low amount of diesel fuel used (25%-35%) results in soot levels below the minimum detection limit of the smoke meter, even in the case with the shortest mixing time available. Finally, it is worthy to note that since the majority of the combustion event takes place during the compression stroke, no strong improvement in fuel consumption is appreciated as diesel SOI is advanced. On the other hand, the increase in GF from 65% to 75% resulted in more delayed combustion with almost equal duration, leading to better fuel consumption while increasing CO, HC and decreasing NOx emissions.

To assess the differences in combustion development between pistons, Figure 5 shows the RoHR traces of the most interesting settings in terms of the relative fuel consumption and emissions of the proposed sweeps for the three piston geometries. In order to associate the represented tests with their experimental emissions and combustion metrics in Figure 3, cross symbols are included there.

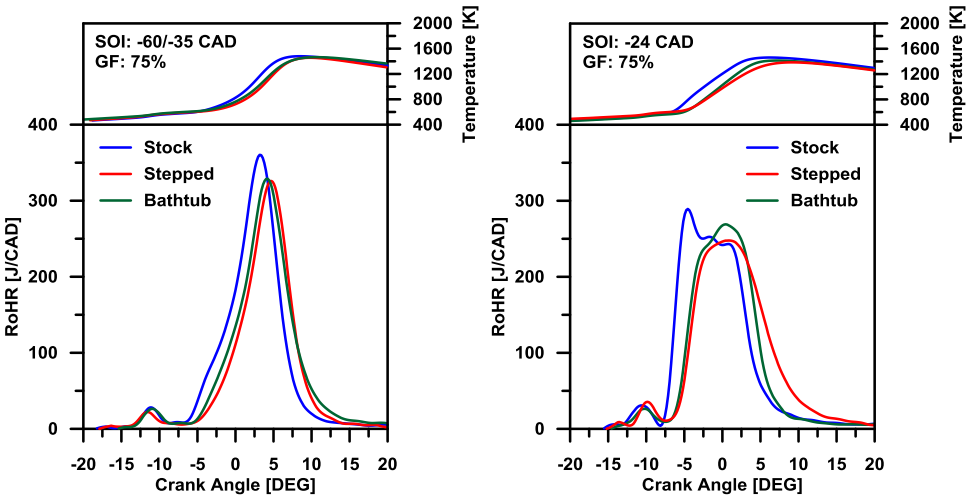

Figure 5. Experimental RoHR and mean temperature of the most interesting tests with double (left) and single injection (right) for the three piston geometries at low load conditions.

Double injection results, in Figure 5, state that the stock piston provides an earlier SOC than the other geometries. It is thought to be related to the diesel main injection stratification in the combustion chamber. Thus, the deeper bowl of the stock piston seems to retain more diesel fuel from the main injection (-35 CAD aTDC) resulting in more reactive equivalence ratios, which enhance the autoignition process. The remarkable higher RoHR peak further confirms this thought. Unfortunately, nearly half of the combustion event develops during the compression stroke, which penalizes the fuel consumption for the stock geometry. Moreover, it is interesting to remark that the maximum combustion temperatures for the two designed geometries are almost equal to the stock one, which should be directly related to the reduced heat transfer losses due to the minimized piston surface area. The comparison of the emissions reveals that double injection strategy allows to meet EURO VI NOx and soot limitations for the three piston geometries. Thus, the main differences between pistons in terms of emissions are related to the CO and HC levels, which are clearly improved for the stock geometry due to the enhanced heat release.

In the case of single injection strategy, it is also confirmed that stock piston leads to more advanced SOC than bathtub and stepped geometries. In addition, steeper RoHR with higher maximum peak is observed. With this injection strategy, the spray mixing has a key role on combustion process, and then, the differences in mixture formation due to the differences in bowl geometry have greater impact on combustion development. Thus, it seems that the stock geometry (with a more pronounced bowl) enhances the charge motion, which results in a faster mixing and earlier autoignition. The higher RoHR is thought to be related to differences in the equivalence ratio stratification at SOC. Regarding fuel consumption, bathtub piston allows an improvement compared to the stock geometry due to the slight delay in combustion development together with the similar maximum RoHR peak. By contrast, the smooth and late burn provided by the stepped piston results in worsen BSFC than the stock piston. Focusing on emissions levels, it is highlighted that only the stepped piston reached EURO VI limits for NOx emissions. However, HC and CO emissions are greater than the ones obtained with the other geometries. Finally, it is worthy to note that soot levels are negligible for all the pistons.

3.2. Medium load results

Figure 6 shows the results in terms of emissions and combustion parameters versus the relative fuel consumption to CDC for the different sweeps proposed in Table 5 (b). In this case, the effects associated to the modification of the different settings are highlighted in the NOx emissions subfigure, based also on bathtub results. It should be remarked that, in order to ensure moderated maximum pressure rise rate peaks and

preserve the engine mechanical integrity when using double injection strategies, the effective compression ratio was lowered to 11:1 by means of advancing the intake valves closing event (early Miller cycle). Thus, an increase in boost pressure from 2.2 to 2.96 bar was required to keep constant the air mass flow between the single and double injection strategies.

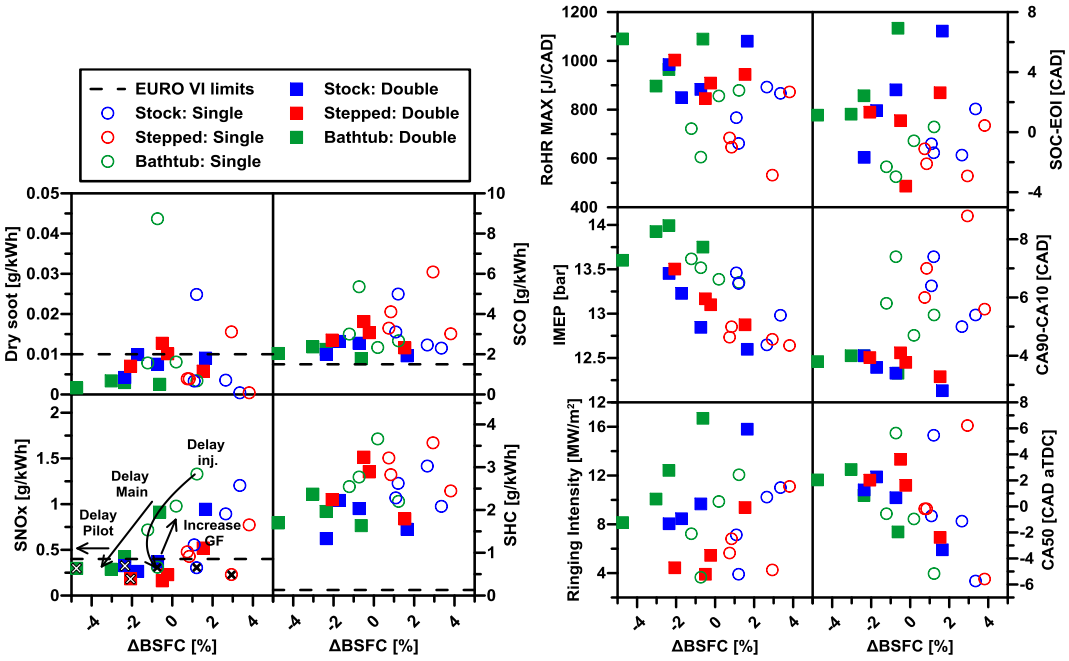

Figure 6. Emissions (left) and combustion parameters (right) for the three piston geometries at medium load conditions versus the relative fuel consumption to CDC. Tests with single and double injection strategies are depicted.

In order to clearly understand the trends presented in Figure 6, the RoHR and mean temperature of the most representative settings in terms of the relative fuel consumption and emissions are shown in Figure 7. As done in the previous section, only the profiles of bathtub piston are depicted.

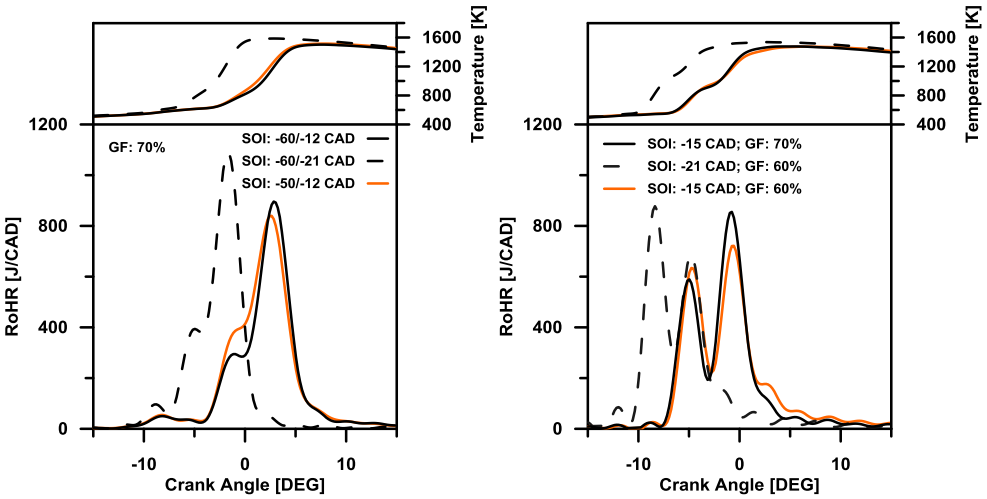

Figure 7. Experimental RoHR and mean temperature of the different sweeps with double (left) and single injection (right) for bathtub piston at medium load conditions.

Concerning the double injection strategy, the same effects found at low load conditions are appreciated. Thus, equal SOC is obtained when advancing the pilot injection from -50 to -60 CAD aTDC. Nonetheless, greater differences in the first RoHR peak are observed at this load. Specifically, the pilot injection set at -50 CAD aTDC improves notably the RoHR in the middle instants of the combustion cycle, leading to improved fuel consumption with lower CO and HC levels. These differences should be related to changes in mixing time, and hence, in the equivalence ratio stratification at SOC. In this sense, the shorter mixing time for the more delayed strategy (-50/-12 CAD aTDC) will provide a richer mixture distribution at SOC. On the other hand, the advance in the main injection from -12 to -21 CAD aTDC results in advanced combustion development with higher in-cylinder temperatures, which leads to higher NOx and lower soot, HC and CO emissions.

Focusing on single injection results, Figure 7 (right) shows well-defined two staged RoHR profiles whatever the injection timing and GF. In this case, the modification in SOI while keeping constant the GF results in opposite behavior in terms of maximum RoHR peaks between the first and second combustion stage. Thus, at the most

advanced case (-21 CAD aTDC), an enhancement of the first premixed phase is appreciated. Moreover, the second RoHR peak becomes lower since great part of the fuel has been already consumed. By contrast, as diesel SOI is delayed, the first RoHR peak becomes lower, which provokes an increase in temperature and pressure resulting in a more powerful autoignition during the second stage. This change in the behavior when SOI is modified is mainly related to the premixed combustion of diesel fuel and the entrained gasoline. Thus, comparing SOC-EOI values in Figure 6, it is confirmed the shorter mixing time in the case of delayed SOI, which promotes lower diesel amount to be burned in premixed manner. Finally, the increase in GF from 60% to 70% at the same SOI enhances the second stage of the combustion development, which results in increased NOx with lower HC and CO emissions.

Figure 8 presents the influence of piston geometry on RCCI combustion at medium load. The double injection strategy at -60/-40 CAD aTDC leads to very similar combustion development for the three geometries. In particular, a combustion pattern similar to the one described at low load conditions is observed. This similitude is explained due to the minor differences among the injection strategies proposed. Focusing on piston comparison, a notable improvement in combustion is achieved with bathtub piston. Moreover, stepped piston also leads to slightly higher RoHR peak compared to the stock geometry. This gain in combustion should be related to the optimized piston surface area for the designed geometries. Concerning performance and emissions, it is clear that the gain in RoHR with bathtub piston leads to remarkable lower BSFC. In addition, it is worthy to remark that this injection strategy also allows to meet EURO VI NOx and soot levels with all the pistons. Finally, HC and CO emissions still remain out of the interesting region, but comparing to low load conditions, the

improvement is clearly confirmed in all cases. In this sense, bathtub piston allows the minimum values, followed by the stock geometry.

Looking at single injection results, a remarkable worsening in combustion development compared with double injection is confirmed whatever the piston geometry. In this sense, the maximum RoHR peaks achieved with single injection were almost 50% lower than the ones reached in double injection tests. This fact, together with the larger combustion duration, resulted in higher HC and CO levels with lower IMEP and RI values. In addition, the negative mixing time (SOC-EOI) for the single injection tests reveals a certain period of diffusion combustion, which leads to unacceptable soot values. Focusing on the represented profiles, it is stated that bathtub and stepped piston provide a slightly delayed and faster combustion than the stock piston, with lower RoHR peak during the second combustion stage. By contrast, bathtub piston leads to higher first RoHR peak and lower BSFC than the stock geometry. In terms of emissions, similar NOx levels are measured for the three pistons. Moreover, CO, HC and soot values are also similar for bathtub and stock geometry, but are slightly higher for stepped piston. This behavior is explained due to the less powerful combustion development, which leads to lower combustion temperatures.

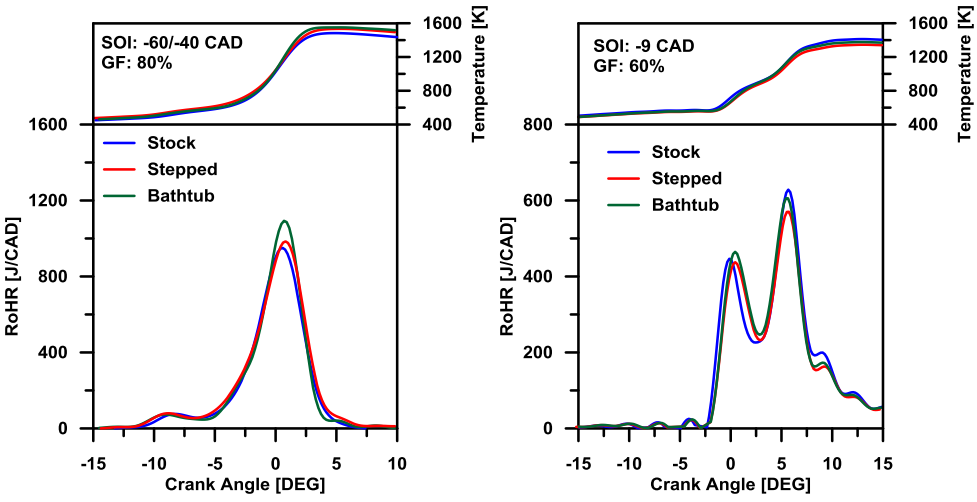

Figure 8. Experimental RoHR and mean temperature of the most interesting tests with double (left) and single injection (right) for the three piston geometries at medium load conditions.

3.3. High load results

The results in terms of emissions and combustion parameters for the tests proposed at high load are presented in Figure 9. The details of the specific sweeps are depicted in Table 5 (c). As done in the previous section, the effects associated to the modification of the different settings are highlighted in the NOx emissions subfigure, taking as reference the bathtub piston. In addition, the effective compression ratio was also lowered to 11:1.

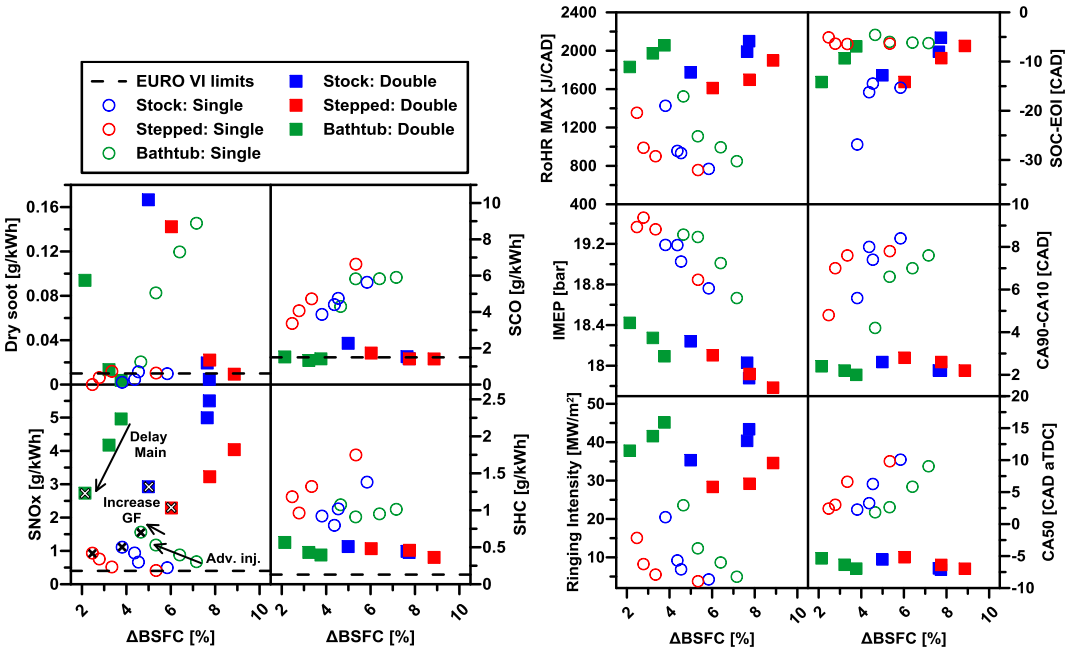

Figure 9. Emissions (left) and combustion parameters (right) for the three piston geometries at high load conditions versus the relative fuel consumption to CDC. Tests with single and double injection strategies are depicted.

As seen in Figure 10, the more advanced achievable value for pilot injection was -40 CAD aTDC because of the unacceptable knocking levels, which are depicted in Figure 9. Therefore, only the effect of main SOI is presented in Figure 10. Comparing the RoHR profiles, it is shown that as main SOI is delayed the combustion development becomes also delayed and weaker. In this sense, the injection event set at -4 CAD aTDC takes place at the end of the combustion process, and then, has a negligible contribution to

the RoHR. In addition, as seen in Figure 9, the diesel fuel amount injected at these instants caused a great impact in soot emissions. Moreover, due to the poor combustion attained, higher CO and HC emissions with lower NOx levels were observed.

Regarding single injection, a double staged RoHR with higher peak in the second stage is observed in all cases. Thus, the advance in SOI from -3 to -9 CAD aTDC provokes an improvement in both combustion phases due to the higher pressure and temperature at these instants of the cycle. Finally, the increase in GF clearly enhances the second combustion stage, where the majority of the gasoline is consumed, while the first stage remains almost unaffected. Thus, both modifications (advance in SOI and increase GF) results in higher NOx and lower soot and unburned products.

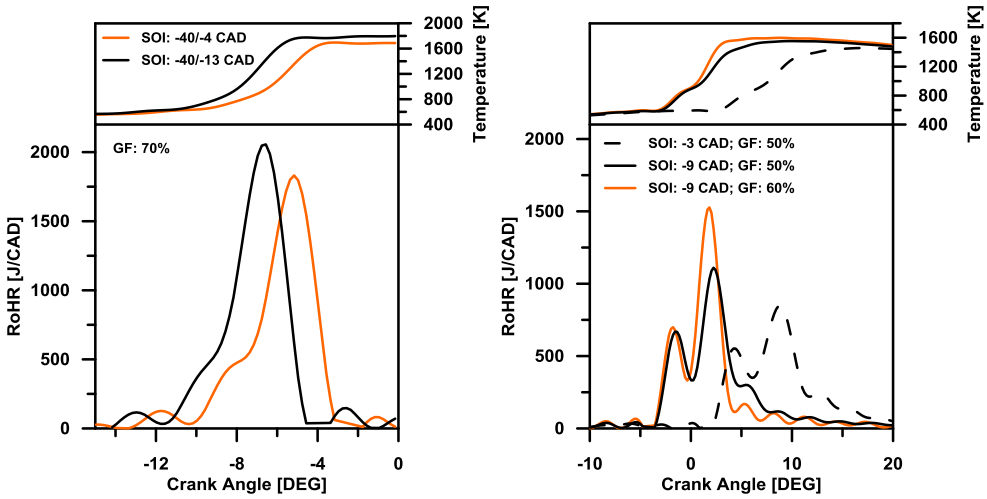

Figure 10. Experimental RoHR and mean temperature of the different sweeps with double (left) and single injection (right) for bathtub piston at high load conditions.

Figure 11 shows the direct comparison between the three geometries using single and double injection strategies at high load. From the double injection results, it is highlighted the notable differences in the first instants of the high temperature heat release. Thus, the stock geometry shows a more progressive increase in the RoHR profile, while stepped and bathtub pistons present an intermediate change in the

RoHR slope. Comparing the combustion metrics in Figure 9, an almost equal mixing time (SOC-EOI), combustion duration (CA90-CA10) and combustion phasing (CA50) are observed for the three pistons. Similar emissions levels are also observed for all the geometries, with the exception of the significant improvement in soot emissions for bathtub piston for the most delayed case. In this sense, since the mixing time is almost equal in all the cases, the differences in soot emissions should be related to the oxidation process. Thus, the greater in-cylinder temperature for bathtub piston should benefit the soot oxidation. It is worthy to note that, contrarily to the findings at low and medium load, the double injection is not a suitable strategy to achieve NOx and soot emissions under EURO VI limits. In addition, unacceptable knocking levels are recorded whatever the piston geometry.

Focusing on single injection results in Figure 9, a general improvement in NOx emissions with respect to double injection is confirmed whatever the piston geometry. Moreover, ringing intensity values are reduced up to 50%. Soot emissions are also minimized for the stock and stepped geometries, but not for bathtub piston. In this case, the excessive shallow geometry of the bowl worsens the charge motion and difficult the mixing process. Also of note is that, stepped piston allows the minimum BSFC, while bathtub piston worsens it with respect to the stock geometry. HC emissions are similar for the three pistons and CO levels are clearly improved with the stepped geometry. This trend is confirmed looking to the RoHR results, which a notable enhancement of the second combustion stage is observed with stepped piston. In this sense, the slight changes in combustion pattern between pistons when using a delayed injection strategy may be related to the interaction of diesel spray with the piston geometries.

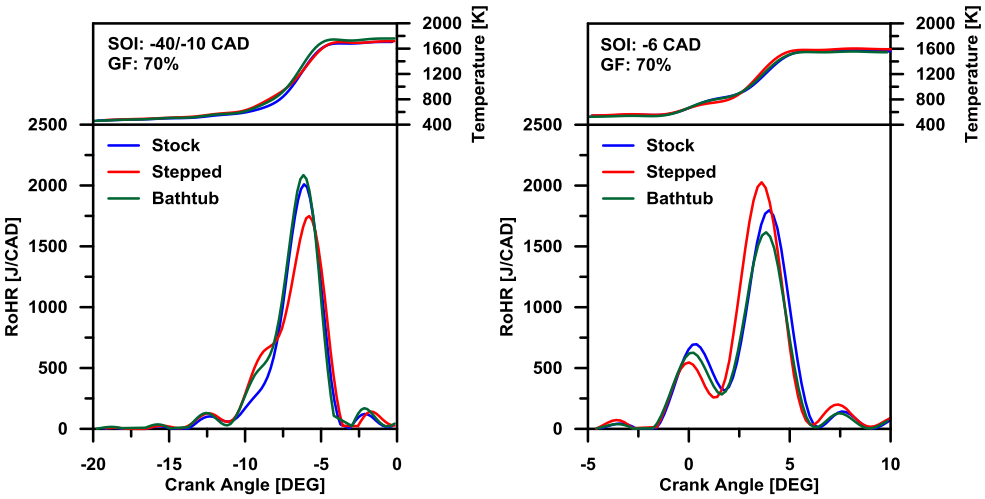

Figure 11. Experimental RoHR and mean temperature of the most interesting tests with double (left) and single injection (right) for the three piston geometries at high load conditions.

4. Discussion

A merit function [44] was used to select the proper engine settings for the different piston geometries and engine loads. The values of the self-imposed constraints used to calculate the merit function were NOx=0.4 g/kWh, soot=0.01 g/kWh, PRR=15 bar/CAD and BSFC=$BSFC_{CDC}$ g/kWh. These limitations were aimed to fulfill EURO VI limits while preserving the engine mechanical integrity and improving fuel consumption with respect to CDC operation. Thus, the contribution to the merit function from a given variable will be zero if only the measured value is less than or equal to the specified limit. When F is non-zero, the contribution from each constrained parameter can be examined separately to quantify the severity of its non-compliance. The merit function is defined as follows:

$$F = \sum_i \max\left(0, \frac{x_i}{x_i^*} - 1\right) \tag{3}$$

If various operating conditions fulfilled all the constraints (which results in a merit function value of zero) for the same piston and load, the best condition was considered the one that minimized the CO and HC emission levels.

Figure 12 shows the merit function results for all the tests carried out in this work. In addition, the selected engine operating conditions together with their merit function value are also marked with a rounded symbol in the figure. As seen from the figure, the selected operating conditions at low and medium load fulfilled all the constraints whatever the piston geometry.

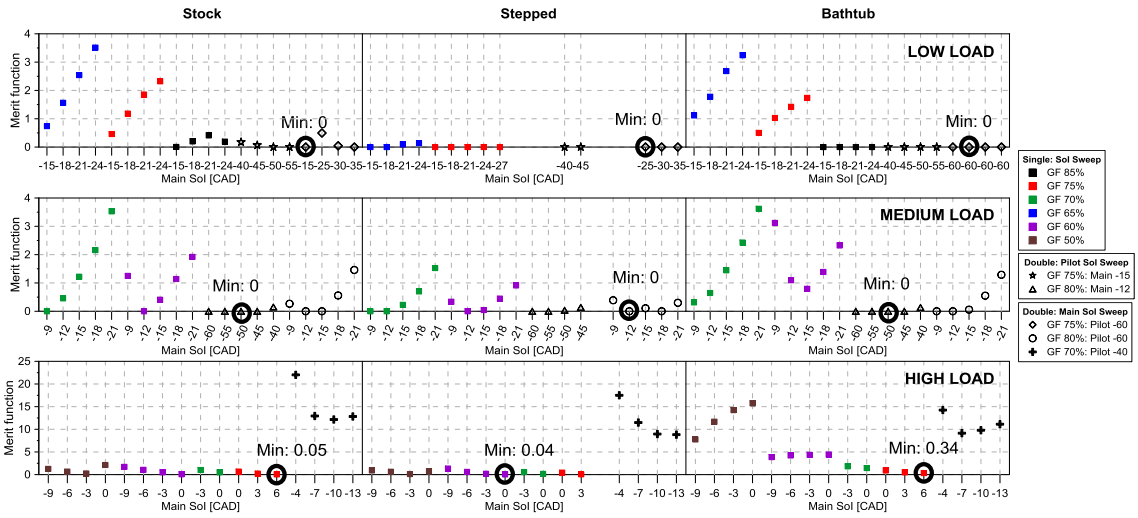

Figure 12. Merit function results calculated taking into account four constraints: EURO VI limits (NOx=0.4 g/kWh and soot=0.01 g/kWh), maximum PRR=15 bar/CAD and BSFC=$BSFC_{CDC}$ g/kWh. The remarked operating conditions correspond to the ones that provide minimum CO and HC emission levels.

To summarize these results, Figure 13 represents NOx, soot, combustion efficiency, BSFC relative to CDC and maximum PRR versus the engine load for the tests previously selected. As seen from the figure, EURO VI NOx levels are reached whatever the piston and engine load. Moreover, the stock and stepped pistons leads also to soot emissions under EURO VI limits for all the engine loads. By contrast, bathtub geometry exceeds the limitation at high load due to the poor mixing process provided by the excessive shallow bowl. On the other hand, stepped piston allows a moderate improvement in BSFC with respect to CDC for the whole operating range, with a decrease in the gain as load is increased. Otherwise, the stock and bathtub geometries provide a remarkable improvement in fuel consumption at low and medium load with a notable penalty at

high load. Finally, it is interesting to remark that the highest combustion efficiency from low to medium load is achieved with the stock geometry, with similar values than stepped piston at high load. In this sense, bathtub piston allows a great improvement in combustion efficiency at high load at the expense of higher NOx, soot and maximum PRR levels.

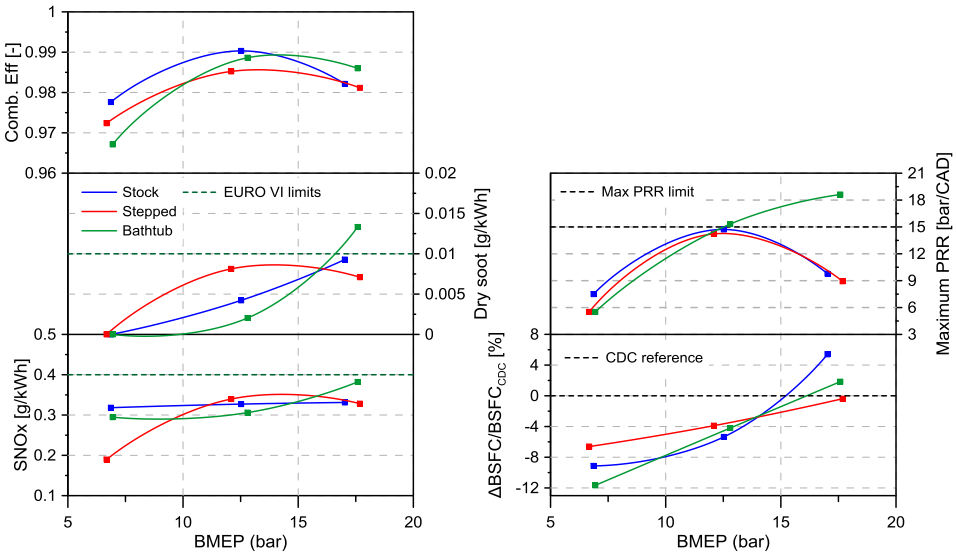

Figure 13. NOx, soot, combustion efficiency, BSFC relative to CDC and maximum PRR versus engine load for the best points of the different pistons.

5. Conclusions

In the present experimental work, three different piston bowl geometries has been tested at the same engine operating points using single and double injection strategies, providing a direct comparison in terms of RCCI performance and emissions from low to high load.

The results at low load, in which the greatest differences in combustion pattern between pistons were observed, showed that the more pronounced bowl of the stock piston enhanced the mixing process providing earlier SOC than bathtub and stepped geometries. In spite of these differences, all pistons allowed ultra-low NOx and soot emissions whatever the injection strategy used. Also, the new geometries resulted in slightly increased CO and HC levels due to the smoother combustion process. By

contrast, at medium load, the reduced heat transfer losses due to the remarkable lower area to volume ratio of bathtub piston promoted higher combustion temperature peaks, which contributed to reduce combustion losses and fuel consumption while maintaining NOx and soot emissions under EURO VI levels. At this engine load, stepped geometry showed similar results than stock piston. Finally, a single injection pattern was required to reach low NOx and soot emissions with moderate pressure rise rates at high load. In this case, stepped piston showed more promising results than the stock and bathtub geometries in terms of NOx, soot and fuel consumption with slight penalty in HC emissions.

The global comparison of the three geometries under certain self-imposed constraints suggested that the more suitable piston geometry to operate under RCCI conditions from low to high load is the stepped one. Despite bathtub piston allowed greater benefits in terms of fuel consumption and soot emissions than stepped geometry up to medium load, the required use of single injection at high load led to unacceptable soot and knocking levels. Thus, as previous literature demonstrates, it has been confirmed that a flat bowl with reduced piston surface area contributes to increase RCCI efficiency. Whereas, under the operating conditions of the current study, bathtub piston is not the most suitable geometry for full operating range. The soot limitation implies that bathtub geometry would not be suitable neither for extending RCCI concept up to full load nor for implementing dual-mode concept, in which convention diesel combustion mode would be used at full load if RCCI concept were not possible.

Acknowledgments

The authors acknowledge VOLVO Group Trucks Technology for supporting this research.

References

[1]Mingfa Y, Zhaolei Z, Haifeng L. Progress and recent trends in homogeneous charge compression ignition (HCCI) engines. Progress in Energy and Combustion Science 35 (5) (October 2009) 398-437.

[2]Maurya R K, Agarwal A K. Experimental study of combustion and emission characteristics of ethanol fuelled port injected homogeneous charge compression ignition (HCCI) combustion engine. Applied Energy, Vol. 88, pp 1169-1180, 2011.

[3]Lu X, Han D, Huang Z. Fuel design and management for the control of advanced compression-ignition combustion modes. Progress in Energy and Combustion Science, 37, 2011:741-783.

[4]Cerit M, Soyhan H S. Thermal analysis of a combustion chamber surrounded by deposits in an HCCI engine. Applied Thermal Engineering 50 (1) (2013) 81-88.

[5]Bessonette P W, Schleyer C H, Duffy K P, Hardy W L, Liechty M P. Effects of fuel property changes on heavy-duty HCCI combustion. SAE paper 2007-01-0191, 2007.

[6]Singh A P, Agarwal A K. Combustion characteristics of diesel HCCI engine: an experimental investigation using external mixture formation technique. Appl Energy 2012. Volume 99, November 2012, Pages 116-125

[7]Law D, Kemp D, Allen J, Kirkpatrick G, Copland T. Controlled combustion in an IC-engine with a fully variable valve train. SAE paper 2001-01-0251; 2001.

[8]Agrell F, Ångström H-E, Eriksson B, Wikander J, Linderyd J. Integrated simulation and engine test of closed loop HCCI control by aid of variable valve timings. SAE paper 2003-01-0748; 2003.

[9]Haraldsson G, Tunestål P, Johansson B, Hyvönen J. HCCI combustion phasing in a multi cylinder engine using variable compression ratio. SAE paper 2002-01-2858; 2002.

[10]Maurya R K, Agarwal A K. Experimental investigation on the effect of intake air temperature and air–fuel ratio on cycle-to-cycle variations of HCCI combustion and performance parameters. Applied Energy, Vol. 88, pp 1153-1163, 2011.

[11]Payri R, García A, Domenech V, Durrett R, Plazas A. An experimental study of gasoline effects on injection rate, momentum flux and spray characteristics using a common rail diesel injection system. Fuel, Volume 97, July 2012, Pages 390–399.

[12]López JJ, García-Oliver JM, García A, Domenech V. Gasoline effects on spray characteristics, mixing and auto-ignition processes in a CI engine under Partially Premixed Combustion conditions. Applied Thermal Engineering, Volume 70, Issue 1, 5 September 2014, Pages 996–1006.

[13]Kalghatgi G T. Auto-ignition quality of practical fuels and implications for fuel requirements of future SI and HCCI engines. SAE paper 2005-01-0239, 2005.

[14]Kalghatgi G, Risberg P, Angstrom H. Advantages of fuels with high resistance to autoignition in late-injection, low-temperature, compression ignition combustion. SAE Trans., 2006, 115(4), 623–634.

[15]Liu H, Yao M, Zhang B, Zheng Z. Effects of inlet pressure and octane numbers on combustion and emissions of a homogeneous charge compression ignition (HCCI) engine. Energy and Fuels, 2008, 22(4), 2207–2215.

[16]Christensen M, Hultqvist A, Johansson B. Demonstrating the multi-fuel capability of a homogeneous charge compression ignition engine with variable compression ratio. SAE paper 1999-01-3679, 1999.

[17]Benajes J, García A, Domenech V, Durrett R. An investigation of partially premixed compression ignition combustion using gasoline and spark assistance. Applied Thermal Engineering, Volume 52, Issue 2, 15 April 2013, Pages 468-477.

[18]Benajes J, García A, Tormos B, Monsalve-Serrano J. Impact of Spark Assistance and Multiple Injections on Gasoline PPC Light Load. SAE Int. J. Engines 7(4):2014, doi:10.4271/2014-01-2669.

[19]Pastor JV, García-Oliver JM, García A, Micó C, Durrett R. A spectroscopy study of gasoline partially 365 premixed compression ignition spark assisted combustion. Appl Energy 2013;104:568–75. 366.

[20]Desantes JM, Payri R, García A, Monsalve Serrano J. Evaluation of Emissions and Performances from Partially Premixed Compression Ignition Combustion using Gasoline and Spark Assistance. SAE Technical Paper 2013-01-1664, 2013, doi:10.4271/2013-01-1664.

[21]Benajes J, Molina S, García A, Monsalve-Serrano J, Durrett R. Conceptual model description of the double injection strategy applied to the gasoline partially premixed compression ignition combustion concept with spark assistance. Applied Energy, Volume 129, 15 September 2014, Pages 1-9.

[22]Benajes J, Molina S, García A, Monsalve-Serrano J, Durrett R. Performance and engine-out emissions evaluation of the double injection strategy applied to the gasoline partially premixed compression ignition spark assisted combustion concept. Applied Energy, Volume 134, 1 December 2014, Pages 90-101.

[23]Splitter D A, Wissink M L, Hendricks T L, Ghandhi J B, Reitz R D. Comparison of RCCI, HCCI, and CDC Operation from Low to Full Load, THIESEL 2012 Conference on Thermo- and Fluid Dynamic Processes in Direct Injection Engines, 2012.

[24]Kokjohn S, Hanson R, Splitter D, Reitz, R. Experiments and Modeling of Dual-Fuel HCCI and PCCI Combustion Using In-Cylinder Fuel Blending. SAE Int. J. Engines 2(2):24-39, 2010, doi:10.4271/2009-01-2647.

[25]Kokjohn S, Musculus M, Reitz R. Evaluating temperature and fuel stratification for heat-release rate control in a reactivity-controlled compression-ignition engine using optical diagnostics and chemical kinetics modeling. Combustion and Flame, 162 (2015) 2729–2742.

[26]Kokjohn S, Reitz R, Splitter D, Musculus M. Investigation of Fuel Reactivity Stratification for Controlling PCI Heat-Release Rates Using High-Speed Chemiluminescence Imaging and Fuel Tracer Fluorescence. SAE Int.J. Engines 5(2):2012, doi:10.4271/2012-01-0375.

[27]Li J, Yang W M, An H, Zhou D Z, Yu W B, Wang J X, Li L. Numerical investigation on the effect of reactivity gradient in an RCCI engine fueled with gasoline and diesel. Energy Conversion and Management, Volume 92, 1 March 2015, Pages 342-352.

[28]Splitter D, Hanson R, Kokjohn S, Wissink M, et al. Injection Effects in Low Load RCCI Dual-Fuel Combustion. SAE Technical Paper 2011-24-0047, 2011, doi:10.4271/2011-24-0047.

[29]Leermakers C, Van den Berge B, Luijten C, Somers L, et al. Gasoline-Diesel Dual Fuel: Effect of Injection Timing and Fuel Balance. SAE Technical Paper 2011-01-2437, 2011, doi:10.4271/2011-01-2437.

[30]Leermakers C, Somers L, Johansson, B. Combustion Phasing Controllability with Dual Fuel Injection Timings. SAE Technical Paper 2012-01-1575, 2012, doi:10.4271/2012-01-1575.

[31]Kokjohn S L, Hanson R M, Splitter D A, Reitz R D. Fuel reactivity controlled compression ignition (RCCI): a pathway to controlled high-efficiency clean combustion, International Journal of Engine Research, 2011. Volume 12, June 2011, Pages 209-226.

[32]Desantes J M, Benajes J, García A, Monsalve-Serrano J. The Role of the In-Cylinder Gas Temperature and Oxygen Concentration over Low Load RCCI Combustion Efficiency. Energy, Volume 78, 15 December 2014, Pages 854–868.

[33]Prikhodko V, Curran S, Parks J and Wagner R. Effectiveness of Diesel Oxidation Catalyst in Reducing HC and CO Emissions from Reactivity Controlled Compression Ignition. SAE Int. J. Fuels Lubr. 6(2):329-335, 2013, doi:10.4271/2013-01-0515.

[34]Zhou D Z, Yang W M, An H, Li J, Shu C. A numerical study on RCCI engine fueled by biodiesel/methanol. Energy Conversion and Management, Volume 89, 1 January 2015, Pages 798-807.

[35]Tutak W. Bioethanol E85 as a fuel for dual fuel diesel engine. Energy Conversion and Management, Volume 86, October 2014, Pages 39-48.

[36]Splitter D A, Reitz R. Fuel reactivity effects on the efficiency and operational window of dual-fuel compression ignition engines. Fuel, Volume 118, 15 February 2014, Pages 163-175.

[37]Şahina Z, Durguna O, Mustafa Kurtb M. Experimental investigation of improving diesel combustion and engine performance by ethanol fumigation-heat release and flammability analysis. Energy Conversion and Management, Volume 89, 1 January 2015, Pages 175–187.

[38]Benajes J, Molina S, García A, Monsalve-Serrano J. Effects of Direct injection timing and Blending Ratio on RCCI combustion with different Low Reactivity Fuels. Energy Conversion and Management, Volume 99, 15 July 2015, Pages 193-209.

[39]Splitter D A, Kokjohn S L, Wissink M L, Reitz R. Effect of compression ratio and piston geometry on RCCI load limits and efficiency. SAE technical paper 2012-01-0383; 2012. http://dx.doi.org/10.4271/2012-01-0383.

[40]Dempsey A, Walker N, Reitz R. Effect of Piston Bowl Geometry on Dual Fuel Reactivity Controlled Compression Ignition (RCCI) in a Light-Duty Engine Operated with Gasoline/Diesel and Methanol/Diesel. SAE Int. J. Engines 6(1):78-100, 2013, doi:10.4271/2013-01-0264.

[41]Kono M, Basaki M, Ito M, Hashizume T, Ishiyama S, Inagaki K. Cooling Loss Reduction of Highly Dispersed Spray Combustion with Restricted In-Cylinder Swirl and Squish Flow in Diesel Engine. SAE Int. J. Engines 5(2):2012.

[42]Payri F, Olmeda P, Martín J, García A. A complete 0D thermodynamic predictive model for direct injection diesel engines. Applied Energy, Volume 88, Issue 12, December 2011, Pages 4632-4641.

[43]Eng J. Characterization of pressure waves in HCCI combustion. SAE paper 2002-01-2859, 2002.

[44]Cheng A, Upatnieks A, Mueller C. Investigation of Fuel Effects on Dilute, Mixing-Controlled Combustion in an Optical Direct-Injection Diesel Engine. Energy Fuels, 21 (4), pp 1989–2002, 2007.

Abbreviations

aTDC: After Top Dead Center

BSFC: Break Specific Fuel Consumption

CAD: Crank Angle Degree

CA10: Crank angle at 10% mass fraction burned

CA50: Crank angle at 50% mass fraction burned

CA90: Crank angle at 90% mass fraction burned

CDC: Conventional Diesel Combustion

CO: Carbon Monoxide

CR: Compression Ratio

DI: Direct Injection

EGR: Exhaust Gas Recirculation

EOI: End of Injection

EVC: Exhaust Valve Close

EVO: Exhaust Valve Open

FSN: Filter Smoke Number

GF: Gasoline Fraction

HC: Hydro Carbons

HCCI: Homogeneous Charge Compression Ignition

HD: Heavy Duty

IP: Injection Pressure

IVC: Intake Valve Close

IVO: Intake Valve Open

LTC: Low Temperature Combustion

ON: Octane Number

PM: Particulate Matter

PFI: Port Fuel Injection

PPC: Partially Premixed Charge

PRR: Pressure Rise Rate

RCCI: Reactivity Controlled Compression Ignition

RoHR: Rate of Heat Release

SOC: Start of Combustion

SOI: Start of Injection

VVA: Variable Valve Actuation